

Fig. 3 Another comparison of the second-order damping moment with experimental values.⁹

(3) was found to be

$$\phi_1^R = -2Kzy\phi_{0x} + M^2\phi_0\phi_{0x} + M^2Nz\phi_{0x}\phi_{0z} \quad (7)$$

Now we can consider the solution ϕ_1 as the sum of the particular solution Eq. (7) and the complementary solution ϕ_1^c that satisfies Eq. (2) and subjects to the boundary condition

$$\phi_1^c(x, y, 0) = \phi_{1z}(x, y, 0) - \phi_1^R(x, y, 0) \quad (8)$$

The damping in roll coefficient Cl_p can be written as

$$Cl_p = (2C^4/Sb^2) \iint_{\text{wing area}} y \Delta C_p / \partial K dx dy \quad (9)$$

Calculations and Discussion

We have calculated the roll damping moments of two rocket models using the linearized and second-order theories. The effects of wingbody interference are estimated by the linearized theory.⁶

Figure 2 is a study of the effect of freestream Mach number on the damping moment of the basic finner in roll. The cross section of its fins is an 8% thick wedge. It presents the values of the Cl_p estimated in this manner as compared to the experimental values presented in Ref. 8. Figure 2 indicates that the agreement between theory and experiment has been improved considerably.

Figure 3 shows the roll damping moment of a rocket model. The calculated results of the linearized and second-order theories were compared with the experimental values presented in Ref. 9. Because of the small thickness of the wings (only about 3%), the use of the second-order theory did not result in much improvement.

Conclusions

Because an exact particular solution Eq. (7) has been found in this Note, a real three-dimensional second-order theory may be used to study the problem of stability of a rolling wing of an arbitrary planform and cross-sectional shape in a supersonic stream. The results show that the second-order theory can give a slight improvement in the roll damping of a wingbody rocket based on the results of the linearized theory.

References

- ¹Van Dyke, M.D., "Study of Second-Order Supersonic Flow Theory," NACA TN 2200, 1951.
- ²Van Dyke, M.D., "A Study of Second-Order Supersonic Flow Theory," NACA Rept. 1081, 1952.
- ³Martin, J.C. and Gerber, N., "The Second-Order Lifting Pressure and Damping in Roll of Sweptback Rolling Airfoils at Supersonic Speeds," *Journal of the Aeronautical Sciences*, Vol. 20, Oct. 1953, pp. 699-704.
- ⁴Qian, F.X. and Gu, W.K., "Accuracy and Application of a Second-Order Theory for Three-dimensional Supersonic and Low Hypersonic Unsteady Flow around a Thin Wing," *Acta Astronautica et Astronautica Sinica*, Vol. 2, No. 1, 1981, pp. 1-9.
- ⁵Gu, W.K., "The Aerodynamic Behavior of A Harmonically Oscillating Delta Wing in Supersonic and Low Hypersonic Flow Including Nonlinear Thickness Effects," *Proceedings of the Third Asian Congress of Fluid Mechanics*, Tokyo, Sept. 1-5, 1986.
- ⁶Lebejeve, A.A. and Gernobrovkii, L.S., *Jinamika Poleta Bepilovnakh Letatel'nykh Apparátov*, Oborongiz, SSSR, 1962.
- ⁷Gu, W.K., "On Second-Order Theory," Div. 15, Institute of Mechanics, Academia Sinica, Beijing, Res. Rept., Feb. 1981.
- ⁸Murthy, H.S., "Subsonic and Transonic Roll Damping Measurements on Basic Finner," *Journal of Spacecraft and Rockets*, Vol. 19, Jan.-Feb. 1982, pp. 86-87.
- ⁹Shirouzu, M. et al., "An Experimental Study on the Induced Rolling Moment due to Wing-Tail Interference and a Roll-controllable Two-Stage Rocket," NAL TR-793, Dec. 1983.

Dynamic Stability Tests on Finned Bodies at Hypersonic Mach Number

G. R. Hutt* and R. A. East†

University of Southampton, Hants, England

Nomenclature

C_m	= pitching moment coefficient = $M_{aero}/\frac{1}{2}\rho V^2 Sd$
$C_{m\alpha}$	= pitching aerodynamic stiffness derivative = $\partial C_m / \partial \alpha$
$C_{m\dot{\alpha}}$	= pitching moment derivative due to rate of change of angle of attack = $\partial C_m / \partial (\dot{\alpha} d / 2V)$
C_{mq}	= pitching moment derivative due to rate of pitching = $\partial C_m / \partial (q d / 2V)$
d	= model centerbody diameter
L	= total model length, nose to cylinder base
M	= freestream Mach number
M_{aero}	= aerodynamic moment
q	= pitch rate of oscillating model
Re_d	= Reynolds number based on cylinder body diameter
S	= cylinder area = $(\pi d^2 / 4)$
V	= flow speed
X_{cg}	= axial distance from the nose tip to the oscillation axis
α	= angle of attack, deg
$\dot{\alpha}$	= rate of change of α w.r.t. time
ρ	= flow density

Received July 25, 1985; revision received Jan. 22, 1986. Copyright © 1986 by G. R. Hutt. Published by the American Institute of Aeronautics and Astronautics, Inc., with permission.

*Lecturer, Aeronautics and Astronautics Department. Member AIAA.

†Professor, Aeronautics and Astronautics Department. Member AIAA.

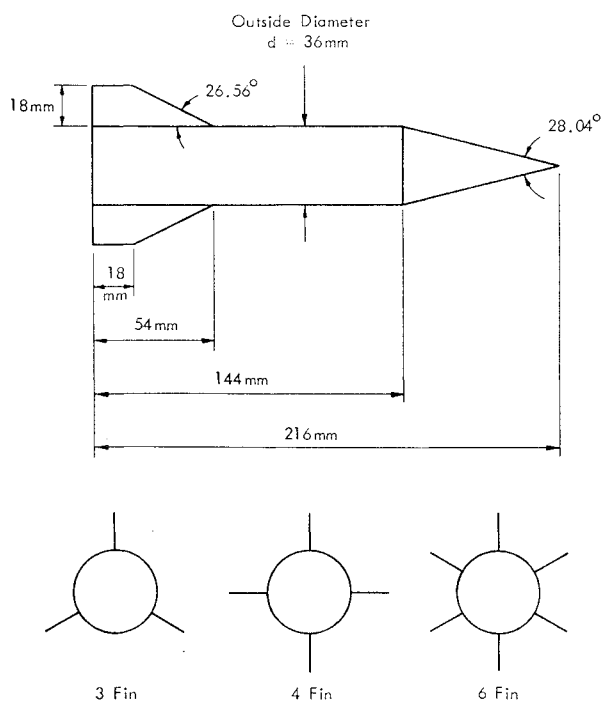


Fig. 1 Model configuration.

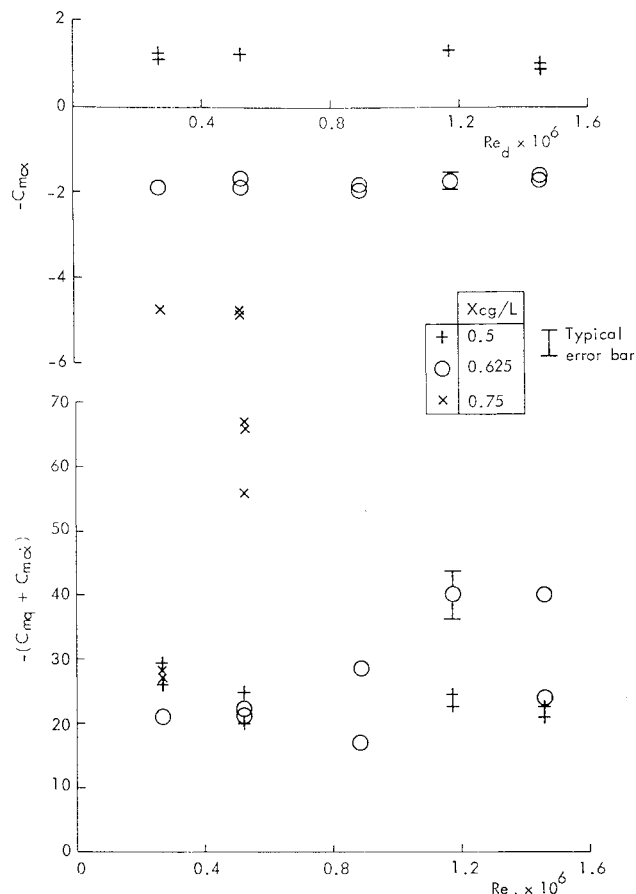
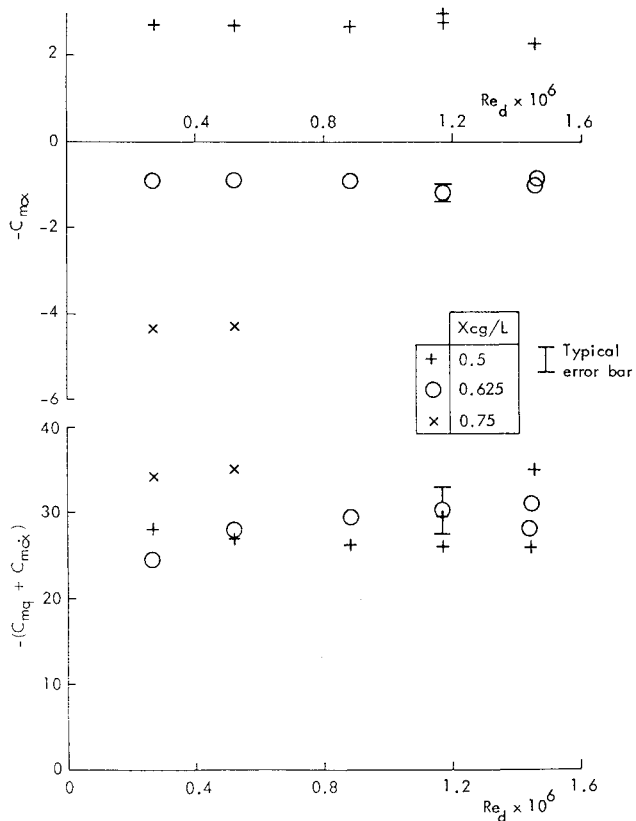
Introduction

STIMULATED by ballistic vehicle research, studies have been made of the high Mach number stability characteristics of axisymmetric projectiles such as cones, ogives, and a hyperballistic series of shapes. However, there is a dearth of experimental data on slender finned vehicles in hypersonic flow. Given the trend of increasing flight Mach number for this type of vehicle, in combination with strong viscous effects on stability observed on finless shapes, it is essential that experimental data on fin and Reynolds number effects on aerodynamic stability be obtained. This paper presents the results of an experimental study to deduce the pitch stability of cone-cylinder bodies with 3, 4, and 6 fins.

Models and Test Conditions

The experimental data presented here were obtained in an isentropic light piston tunnel at the University of Southampton. This is an intermittent facility providing a 0.21-m-diam open jet flow of $M = 6.85$ for duration of typically 0.5 s. Further details of the wind tunnel are given by East and Qasrawi.¹ As shown in Fig. 1, the common part of the test vehicle is a pointed cone nose and a cylindrical afterbody with an overall length-to-diameter ratio of 6:1. Data were obtained for 3, 4, and 6 fin configurations and for oscillation axis stations, given by X_{cg}/L , of 0.5, 0.625, and 0.75. The fins are symmetric in cross section with a 15 deg angle chamfer relative to the fin plate and normal to its leading edge. The chosen fixed roll angle corresponds to one fin aligned in the pitch plane.

Static (stiffness) and dynamic stability (damping) derivatives, $-C_{m\alpha}$ and $-(C_{mq} + C_{m\dot{\alpha}})$, respectively, were obtained using a sting support dynamic stability rig. The small amplitude free oscillation test technique was employed and the model motion time histories were recorded via an optical model position detector.² The initial model oscillation amplitude was approximately ± 1 deg on a flexure pivot of about zero angle of attack. Throughout the test program the Mach number was fixed at 6.85 and the flow Reynolds number varied by altering the upstream stagnation pressure. The Reynolds number range, based on cylinder body diameter, was $0.27 \times 10^6 \leq Re_d \leq 1.45 \times 10^6$ and the flow stagnation temperature was 600 K.

Fig. 2 Stability derivatives vs Reynolds number for the four-fin model, $L/d = 6$, $M = 6.85$, $\alpha = 0$.Fig. 3 Stability derivatives vs Reynolds number for the six-fin model, $L/d = 6$, $M = 6.85$, $\alpha = 0$.

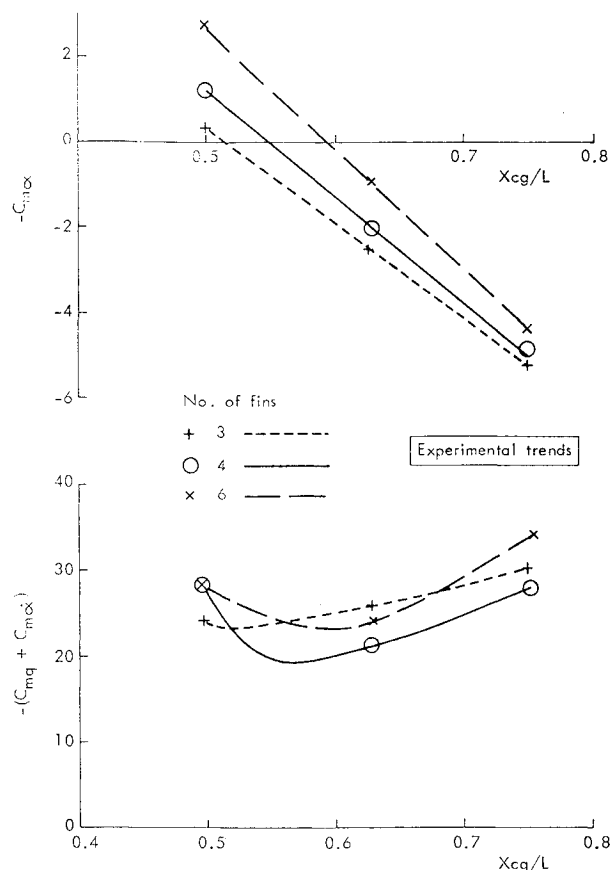


Fig. 4 Stability derivatives vs CG position, $L/d=6$, $M=6.85$, $Re_d=0.27 \times 10^6$, $\alpha=0$.

Results

The variation of the measured stability derivatives for a range of Reynolds numbers for the 3, 4, and 6 fin configurations are shown in Figs. 2, 3, and 4.

For the three-finned configuration data, the stiffness derivatives are independent of the Reynolds number over the range tested. The model with an oscillation axis $X_{cg}/L=0.5$ is statically stable, and, as expected, aft oscillation axis movement promotes static instability. The damping derivative is of the order $-(C_{mq} + C_{m\dot{\alpha}}) = 20 \sim 30$, with the aft oscillation axis yielding the larger values within this range. Similar to the three-fin data, the four-fin stiffness derivative $-C_{m\alpha}$ shown in Fig. 2 is independent of Reynolds number effects. However, the damping derivative $-(C_{mq} + C_{m\dot{\alpha}})$ shows an increase with increased Reynolds number. This increment occurs at lower Reynolds number as the oscillation axis is moved rearward. This phenomena is thought to be due to a viscous crossflow affecting transitional flow. With the exception of the model with an oscillation axis $X_{cg}/L=0.75$, the damping derivative is of the order, $-(C_{mq} + C_{m\dot{\alpha}}) = 20 \sim 40$. Although the data for the models with an increase in fin number show an increase in stiffness derivative, only the model with the oscillation axis at $X_{cg}/L=0.5$ is statically stable. The six-fin model data, shown in Fig. 3, indicate that the stiffness derivative is Reynolds number independent. The damping derivative data show some increase with Reynolds number, in the range $-(C_{mq} + C_{m\dot{\alpha}}) = 25 \sim 35$, which is also related to axis position. Experimental data trends for $L/d=6$ model $Re_d=0.27 \times 10^6$ are presented as a function of oscillation axis location in Fig. 4. The observed trends clearly show the decrease in static stability $-C_{m\alpha}$ with rearward oscillation axis location in combination

with increased static stability increased fin number. The dynamic derivative, with $-(C_{mq} + C_{m\dot{\alpha}})$, trends identify characteristic minima which accompany the respective axial center-of-pressure locations along the model axis where $-C_{m\alpha}=0$. The lowest damping derivative is that of the four-finned model.

Transitional boundary-layer effects on slender vehicle stability at hypersonic Mach numbers have been widely reported, for example, by Ericsson.³⁻⁵ Experiments conducted in the Southampton hypersonic wind tunnel⁶ show that for Reynolds numbers equivalent to $Re_d > 1.16 \times 10^6$, a pointed 10-deg cone is subject to transitional flow on the aft body. At the lowest values of test Reynolds number, the flow over the slender finned bodies tested here is most likely to be laminar. Increasing Reynolds number promotes an increase in damping derivative. The Reynolds number at which this occurs is dependent on the fin number and oscillation axis position. Usually, angle-of-attack-dependent changes in slender vehicle stability derivatives invoke changes in both stiffness and damping derivatives. In this case, however, it is only the damping derivative that is affected. Noting the previously reported^{3,4} sensitivity of slender vehicle stability to viscous effects, it is postulated that the phenomenon responsible is an $\dot{\alpha}$ rate-dependent forebody-viscous crossflow, which subsequently determines the aft body fin effectiveness. It is only the rate term $\dot{\alpha}$ which can decouple the stiffness and damping derivatives, since the $-C_{m\alpha}$ and C_{mq} terms are quasisteady in nature.

Concluding Remarks

The reported experimental data quantify the magnitude of fin number, Reynolds number, and oscillation axis effects on the pitch static and dynamic stability for a finned pointed cone-cylinder geometry in hypersonic flow, at zero mean angle of attack. At low Reynolds numbers, conventional pitch stability-oscillation axis relationships are observed. Also in this regime, incremental effects on pitch static stability with increase in fin number are found, but the consequent changes in the measured dynamic stability are relatively small. A Reynolds number axis position effect on the damping derivative is observed, leading to a suggestion of angle-of-attack rate dependent, $\dot{\alpha}$, viscous flowfield contributions.

Acknowledgment

This work was supported by the Procurement Executive, Ministry of Defence.

References

- ¹East, R. A. and Qasrawi, A. M. S., "A Long Stroke Isentropic Light Piston Tunnel," Aeronautical Research Council Reports and Memorandum, No. 3844, 1978.
- ²Hutt, G. R. and East, R. A., "Optical Measurement Techniques used in Dynamic Wind Tunnel Testing," *Journal of the Institute of Measurement and Control*, Vol. 18, March 1985, pp. 99-101.
- ³Ericsson, L. E., "Effect of Boundary Layer Transition on Vehicle Dynamics," *Journal of Spacecraft and Rockets*, Vol. 6, Dec. 1969, pp. 1404-1409.
- ⁴Ericsson, L. E., "Transition Effects on Slender Vehicle Stability and Trim Characteristics," *Journal of Spacecraft and Rockets*, Vol. 11, Jan. 1974, pp. 3-11.
- ⁵Ericsson, L. E., "Modification of Aerodynamic Prediction of the Longitudinal Dynamics of Tactical Weapons," Lockheed Missiles and Space Company, Sunnyvale, CA, LMSC-D646354, 1979.
- ⁶Khalid, M., "A Theoretical and Experimental Study of the Hypersonic Dynamic Stability of Blunt Axisymmetric Conical and Power Law Shaped Bodies," Ph.D. Thesis, University of Southampton, Hants, UK, 1977.